



Preparation of magnetic rice husk carbon nanocomposite for efficiently extracting aflatoxin B1 from rice followed by time-resolved fluorescent immunochromatographic assay

Di Yuan^{a,b,c}, Bin Hong^{a,b,c}, Shan Zhang^{a,b,c}, Shan Shan^{a,b,c},
Jingyi Zhang^{a,b,c}, Chuanying Ren^{a,b,c,*}

^a Food Processing Research Institute, Heilongjiang Academy of Agricultural Sciences, Harbin 150086, China

^b Heilongjiang Province Key Laboratory of Food Processing, Harbin 150086, China

^c Heilongjiang Province Engineering Research Center of Whole Grain Nutritious Food, Harbin 150086, China

ARTICLE INFO

Keywords:

Aflatoxin B1 (AFB1)
Magnetic solid-phase extraction (MSPE)
Quantification
Time-resolved fluorescent
immunochromatographic assay (TRFICA)
Magnetic rice husk carbon nanocomposite

ABSTRACTS

An on-site, sensitive, and cost-effective method for determining aflatoxin B1 (AFB1) in rice samples is proposed, combining magnetic solid phase extraction (MSPE) and time-resolved fluorescence immunochromatography (TRFICA) techniques. Cost-effective rice husks were carbonized and combined with nanomaterials to make magnetic nanocomposites that acted as effective adsorbents in MSPE. Under optimal conditions, the entire process was completed in 15 min with a visual detection limit of 0.16 µg/kg. Recoveries ranged from 85.2 % to 109.4 %, with intra- and inter-day precisions below 11.5 %. The proposed MSPE-TRFICA method offers a viable alternative for the rapid and highly sensitive quantitative detection of AFB1 for quality assurance.

1. Introduction

Rice (*Oryza sativa*) meets two-thirds of the recommended daily calorie intake and is abundant in vital components (including proteins, carbohydrates, and vitamins), making it an important cereal crop worldwide (Yu et al., 2021). Rice grows in warm, humid environments and is particularly susceptible to contamination by *Aspergillus flavus*, which generates aflatoxin, a secondary metabolite. Aflatoxins can contaminate rice and its associated products during several phases, including harvesting, storage, transportation, and processing (Lai et al., 2015). In 1993, the International Agency for Research on Cancer (part of the World Health Organization) classified aflatoxin B1 (AFB1), as a class I carcinogen, underscoring it as a significant health hazard (Somsuabwin et al., 2018). AFB1 is the most dangerous of the diverse and structurally distinct aflatoxins, and can cause severe cytotoxicity, immunotoxicity, teratogenicity, and carcinogenicity in humans, posing a major threat to human health (Jallow et al., 2021). As a significant contaminant affecting the quality and safety of rice, AFB1 poses a serious hazard to human health, depletes food resources, and significantly restricts the export trade of rice (Yu et al., 2018). The overall prevalence of mycotoxins in rice is about 15 %, with the common mycotoxins being total

aflatoxins (56 %) and AFB1 (34 %) (Chandravarnan et al., 2024). Countries with high rice production face a significant challenge because the high prevalence of AFB1 contamination has several detrimental consequences, including rendering rice unmarketable, causing economic losses, tarnishing of the industry's reputation, and decreasing opportunities for international trade. Consequently, it is imperative for these countries to devote considerable attention to AFB1 contamination and implement effective measures. Countries worldwide and global organizations have enacted rigorous maximum residue limits (MRLs) to monitor and control AFB1 contamination in rice. The MRL for AFB1 in rice is 20 µg/kg in the US, 10 µg/kg in China and Japan, and 2 µg/kg in the European Union (Wu et al., 2023). Given the existing regulatory framework coupled with rigorous survey protocols for rice, it is vital to devise streamlined and highly sensitive methods to detect AFB1.

A diverse array of instrumental methods has been developed for the quantification of AFB1, including sophisticated methods such as high-performance liquid chromatography (HPLC) (Yu et al., 2018), liquid chromatography/tandem mass spectrometry (LC-MS/MS) (Li, Xu, et al., 2022), and electrochemical sensors (Huang et al., 2022). Most of these analytical methods require labor-intensive and time-consuming pre-treatment in the laboratory environment and are unable to rapidly,

* Corresponding author at: Food Processing Research Institute, Heilongjiang Academy of Agricultural Sciences, Harbin 150086, China.

E-mail address: prima365@foxmail.com (C. Ren).

<https://doi.org/10.1016/j.fochx.2024.102145>

Received 3 September 2024; Received in revised form 16 December 2024; Accepted 28 December 2024

Available online 31 December 2024

2590-1575/© 2024 The Author(s). Published by Elsevier Ltd. This is an open access article under the CC BY-NC-ND license (<http://creativecommons.org/licenses/by-nc-nd/4.0/>).

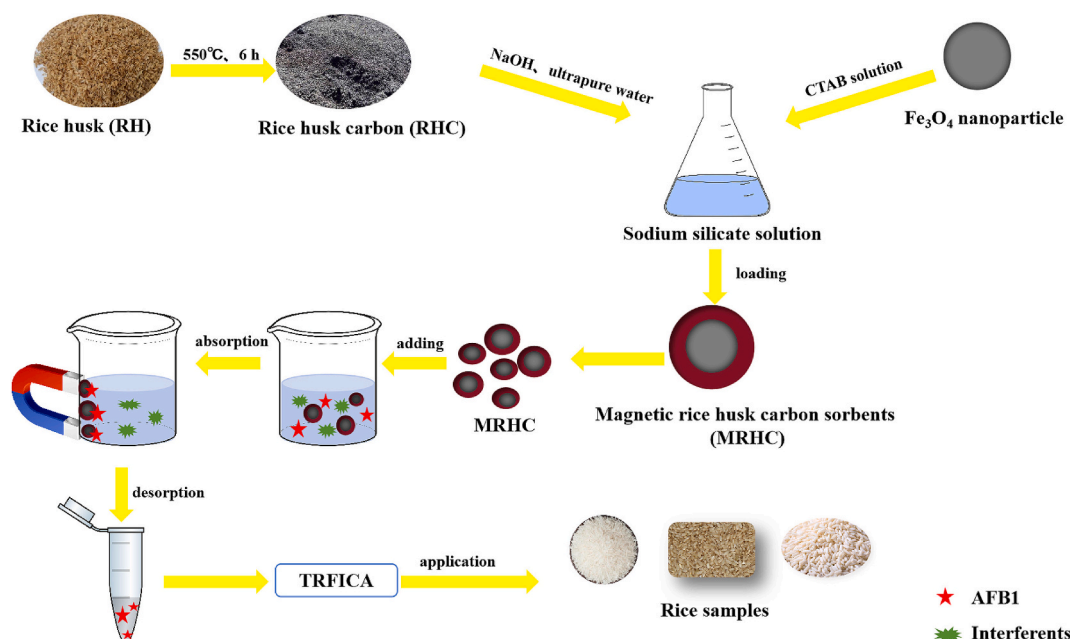


Fig. 1. Schematic illustration of the synthesis and application of MRHC.

sensitively, and accurately detect AFB1 in rice. In addition, immunological detection methods, including enzyme-linked immunosorbent assay (ELISA) (Cao et al., 2024) and colloidal gold immunochromatography (Hu et al., 2018), can be used to analyze the AFB1 content. As an alternative to conventional immunochromatographic techniques, the time-resolved fluorescence immunochromatography assay (TRFICA) has garnered widespread attention because of the approximately 10^3 -fold amplification of the detection signal and its excellent stability (Urusov et al., 2019).

To attain optimal sensitivity levels while simultaneously mitigating matrix effects, a diverse array of solvents and adsorbents have been used in pretreatment steps, such as solid-phase extraction (Yu et al., 2018), application of immunoaffinity columns (Xie et al., 2015), and immunomagnetic solid-phase extraction (Yuan et al., 2023). Most of these pretreatment processes are time consuming and require large amounts of organic solvents and expensive antibodies, which render them unsuitable for application in rice quality screening. In recent years, magnetic solid-phase extraction (MSPE) techniques that leverage magnetic carbonaceous materials have attracted considerable attention for sample pretreatment because of their simple operation steps, time efficiency, and environmental friendliness, and have become a hot topic in analytical chemistry (Özdemir et al., 2019). Novel nanomaterials exhibit great potential in MSPE pretreatment, thereby offering new avenues for the rapid and sensitive detection of AFB1 (Bhat et al., 2022). Magnetic carbon-based materials have both the adsorption capacity of carbon-based materials and the separation properties of magnetic materials, which can quickly separate the adsorbent from the sample matrix, making them highly efficient materials for pretreatment enrichment and purification material (Li, Zhang, et al., 2022). Consequently, magnetic carbon-based materials have been widely utilized in the identification and quantification of pesticides and veterinary medicines, alongside numerous small-molecule pollutants in complex matrices (Senosy et al., 2020).

Rice husk (RH), a by-product of rice manufacturing, is primarily burned on arable land, causing resources wastage and severely polluting the environment (Amran et al., 2021). Rice husk carbon (RHC) is a product obtained from the combustion of rice husk, with a yield of approximately 20 %. It mainly composed of amorphous silica (>98 %), which is highly reactive and can replace the expensive tetraethoxysilane as a natural source of silica (Asadi et al., 2021). Compared to other

adsorbent feedstocks that require mining or processing, the utilization of rice husks for the production of RHC demonstrates superior sustainability. The production process is straightforward and utilizes an abundantly available agricultural waste, and poses no risk of secondary environmental contamination when subjected to appropriate treatment. The exteriorly positioned Si-OH moieties on the RHC exhibited pronounced reactivity, enabling their functionalization through the incorporation of active groups onto either the pore surfaces or skeletal structure. By undergoing magnetization, RHC is transformed into an efficient MSPE adsorbent, characterized by a substantial specific surface area and an abundance of active sites that plays a pivotal role in the pretreatment phase of aflatoxin B1 detection in rice, and is facilitated by the application of a magnetic field.

In this study, we prepared a nanomaterial, a magnetic rice husk carbon adsorbent (MRHC), by utilizing rice husk, a renewable agricultural waste, and introducing Fe₃O₄ nanoparticles to endow it with magnetic properties. The MRHC served as the feedstock for MSPE (Fig. 1). Furthermore, nanomaterials played a pivotal role in purifying the environment and enhancing the efficiency of resource utilization. (Muthukumaran et al., 2022). Subsequently, these synthesized adsorbents underwent rigorous characterization, and the MSPE parameters that influence their extraction efficiency were methodically optimized. By integrating the optimized MSPE process with TRFICA, an expeditious, sensitive, and routine method for quantifying AFB1 in rice was developed.

2. Materials and methods

2.1. Chemicals

Dichloromethane, acetonitrile (CH₃CN), and methanol (MeOH) of HPLC-grade were acquired from Fisher Scientific (St. Louis, USA). Cetyltrimethylammonium bromide (CTAB, analytical reagent grade, ≥99 % purity), APTES (analytical reagent grade, ≥98 % purity), alongside miscellaneous analytical-grade chemicals and reagents, were sourced from Sinopharm Chemical Reagent (Shanghai, China). RH and rice were acquired from a local market (Harbin, China) and subsequently stored at room temperature. The TRFICA testing strips and the accompanying portable reader were supplied by Xiongtu Biotechnology Co. Ltd. (Shanghai, China). Prior to use, all available reagents met or

surpassed analytical standards, eliminating the need for further purification.

2.2. Standards

AFB1 with $\geq 98\%$ purity was procured from Sigma-Aldrich Co., Ltd. (Shanghai, China). A freshly concocted standard stock solution was crafted by accurately measuring $5.0 \text{ mg} \pm 0.1 \text{ mg}$ of the AFB1 reference material and subsequently dissolving it in exactly 1 mL of acetonitrile. To generate a series of standard solutions, the stock solution was diluted with purified water to attain desired concentrations. These prepared standard solutions were stored in the dark at 4°C until the time of utilization.

2.3. Sample preparation

All rice specimens were ground into fine powder until they passed through a 0.85 mm filter. Subsequently, precisely 2 g of this homogenized powder were meticulously weighed into individual centrifuge tube. An aliquot of 2 mL of methanol/water solution, consisting of a 70:30 volume ratio, was introduced into each tube and vigorously agitated for a duration of 3 min using high-speed vortex mixing equipment. Following centrifugation at 3500 rpm for a period of 2 min, a precise 1 mL of resulting supernatant was carefully dispensed into a clean tube, which was subsequently diluted with water to a final volume of 10 mL. The entire extraction process was replicated three times for each sample utilizing the optimized MSPE method.

2.4. Preparation of magnetic rice husk carbon sorbents

Magnetic rice husk carbon sorbents were synthesized according to a previously described manufacturing protocol (Li et al., 2020). RH (200 g) was purified using ultrapure water and dried. After sufficient pulverization, the RH was boiled in 1 L of an HCl (2.0 mol/L concentration) for 2 h to eliminate residual metallic impurities. The precipitate was meticulously rinsed with ultrapure water and dried thoroughly. The dried material underwent calcination at 550°C for 6 h. Subsequently, the resulting carbonized material (11.8 g) and NaOH (14.75 g) were precisely weighed and comprehensively dissolved in 500 mL of ultrapure water, and thereafter heated to 80°C to produce a sodium silicate solution (pH 12).

Fe_3O_4 nanoparticles were synthesized using a coprecipitation technique (Hong et al., 2008). Deionized water (150 mL) and $\text{N}_2\text{H}_4\cdot\text{H}_2\text{O}$ (2 mL) were put into a three-necked 250 mL round-bottom flask equipped with a mechanical stirrer and stirred for 30 min to eliminate oxygen. Subsequently, aqueous solutions of FeCl_3 and FeSO_4 , maintained at a $\text{Fe}^{3+}/\text{Fe}^{2+}$ molar ratio of 1.75:1, were introduced into the flask. Immediately thereafter, 8 mL of aqueous ammonia (25 % v/v) was rapidly injected into the mixture under vigorous stirring conditions. The resultant solution was held at a temperature of 80°C for an additional 30 min. Following this step, the precipitate was meticulously filtered and washed ten times with both deionized water and anhydrous ethanol. The precipitate was then dried under vacuum conditions for 24 h and subsequently ground to a finer powder. Subsequently, the magnetic Fe_3O_4 nanoparticles (400 mg) were added to a 200 mL solution of CTAB (0.02 mol/L) and sonicated for 0.5 h. The mixture was heated to 80°C under magnetic stirring, and 100 mL of sodium silicate solution was then added gradually. After continuous stirring for 0.5 h, the pH of the solution was modulated to 11 through the dropwise addition of 1 mol/L HCl solution, followed by extended stirring for 2 h. Subsequently, the reaction mixture was reacted at 80°C for 24 h. The resulting precipitate was subjected to triple rinsing with ultrapure water to yield the initial product, which was then dried at 50°C . To eliminate surfactant molecules, the dried product underwent calcination at 550°C for 2 h, and the MRHC was finally obtained as powder.

2.5. Characterization of magnetic rice husk carbon sorbents

The magnetic characteristics of the sorbents were documented utilizing the PPMS-9 Vibrating Sample Magnetometer (VSM, Quantum Design, USA). The dimensions of the particles were measured by means of the Hydro 2000SM laser diffraction-based particle sizing apparatus (Mastersizer, United Kingdom).

The Fourier Transform Infrared (FT-IR) absorption spectra were systematically captured on a Shimadzu IRSpirit spectrometer (Shimadzu, Japan) with KBr pellets, the measuring wavenumber range is 400 to 4000 cm^{-1} (Zafar et al., 2021). X-ray Diffraction (XRD) analysis was conducted on a powder diffractometer (Rigaku D/MAX-2600, Japan), operating at 40 kV and 150 mA, furnished with a $\text{Cu-K}\alpha$ radiation emitter emitting a wavelength of 0.154 nm (Syuhada et al., 2021). A systematic acquisition of diffraction profiles was acquired within a 2θ angular range spanning from 5° to 80° , at a scanning velocity of 0.02 s^{-1} . The specific surface area and porous structure were investigated by a Micromeritics ASAP 2460 instrument (Micromeritics, Norcross, GA, USA) based on Brunauer-Emmett-Teller (BET) and Barrett-Joyner-Halenda (BJH) models (Ma et al., 2023).

2.6. MSPE procedure

The MSPE procedure was completed as previously outlined, with minor modifications (Yuan et al., 2023). Briefly, 2 mL of dichloromethane was vortexed with 10 mg of MRHC in a 15 mL centrifuge tube for a duration of 2 min. After discarding the dichloromethane, 10 mL of diluted sample extract was incorporated into the tube. Subsequent vigorous vortex mixing for 3 min, the analyte was prompt adsorbed onto the sorbent material. The MRHC, now laden with AFB1, underwent magnetic separation, and the resulting supernatant was discarded. Thereafter, a 1 min vortex was applied to desorb the analyte using 1 mL of MeOH. The eluting solution was subsequently collected and dried via a nitrogen stream. The remaining residue was reconstituted in 150 μL of ultrapure water, facilitating its analysis via the TRFICA method.

2.7. Adsorption kinetics

MRHC prepared under optimal conditions was utilized to investigate the effect of adsorption time on the adsorption capacity per unit of AFB1 in rice sample extracts. A mixture containing 2 mL of rice sample extract and 18 mL of purified water was prepared, and AFB1 was added to attain a system solution concentration of $2 \mu\text{g/mL}$. This solution was then introduced into a sample vial containing 20 mg of MRHC. The vial was vortexed at 250 rpm at room temperature (25°C) using a platform shaker. At predefined intervals, 1 mL aliquots of the solution were collected, filtered through a $0.22 \mu\text{m}$ membrane, and analyzed for AFB1 content via HPLC. The sorption quantity and adsorption rate were calculated by following equations:

$$Q_t = \frac{(C_0 - C_t)V}{m} \quad (1)$$

$$\text{AFB1 adsorption rate} = \frac{(C_0 - C_e)}{C_0} \times 100 \quad (2)$$

Q_t (mg/g) represents the sorption capacity per milligram of adsorbent at the specific time point t (min). The initial concentration of AFB1 is denoted by C_0 ($\mu\text{g/mL}$), while C_t ($\mu\text{g/mL}$) signifies the AFB1 concentration at time t . Additionally, V (mL) stands for the volume of the solution, and m (mg) indicates the mass of the sorbent utilized.

2.8. TRFICA analysis

In a nutshell, a volume of 50 μL of the adequately prepared solution were mixed with the europium (III) nanoparticle monoclonal antibody in a centrifuge tube. Following a 5 min incubation period at 37°C , a

TRFICA strip was inserted and allowed to incubate for an additional 5 min under the same temperature conditions. Thereafter, the portable reader was fixed at the wavelengths of 365 ± 10 nm and 610 ± 10 nm, enabling the quantification of AFB1 through the employment of quantitative calibration, which relied on the comparative analysis of fluorescence peak area ratios between the test line (T line) and the control line (C line) (Yuan et al., 2023).

2.9. Comparison between SPE-UHPLC-MS/MS and MSPE-TRFICA methods for detecting aflatoxin B1 in rice

To substantiate the MPSE-TRFICA analytical approach, a comparative assessment of the quantitative outcomes derived from TRFICA and UHPLC-MS/MS methodologies was undertaken. A comprehensive array of rice samples fortified with AFB1 concentrations spanning 2 to 10 $\mu\text{g/kg}$, were subjected to quantification utilizing the IAC-UHPLC-MS/MS, a benchmark method. Prior to analysis, sample extracts underwent purification procedures involving immunoaffinity columns. Subsequently, these purified extracts were interrogated by a UHPLC-MS/MS 8050 instrument (Kyoto, Japan), equipped with an electrospray ionization source functioning under positive ionization conditions. The UHPLC-MS/MS instrument comprises a triple quadrupole mass spectrometer with LC-30 CE chromatographic system. Chromatographic separation was executed at a temperature of 40°C , utilizing a Hypesil gold C18 column ($100\text{ mm} \times 2.1\text{ mm}$, $3\text{ }\mu\text{m}$). The mobile phase system comprised A, a 5 mmol/L aqueous ammonium acetate solution, and B, a 1:1 mixture of methanol and acetonitrile. An 5 min isocratic elution protocol employing a 30 % B mobile phase composition was adopted. The volumetric flow rate for the mobile phase was established as 300 $\mu\text{L/min}$, and 1 μL extracted sample was subsequently analyzed utilizing the UHPLC-MS/MS system.

2.10. Method validation

To assess the analytical method, key parameters of MSPE-TRFICA, its standard calibration, precision, and reproducibility, were evaluated. The calibration curve was constructed by the blank rice being spiked with AFB1 at concentrations ranging from 0.5 to 25 $\mu\text{g/kg}$. This curve was subsequently established by the natural logarithm of AFB1 concentrations, utilizing the ratio of the T line and C line intensities. To calculate the visual limit of detection (LOD), 20 blank rice samples were subjected to quantification via the established standard calibration. The limit of quantification (LOQ) was derived by multiplying the LOD by a factor of three (Bai et al., 2021). Under optimal conditions, the accuracy of the method was assessed in terms of its veracity, a metric quantifying systematic deviations, which was computed as the average recoveries. A batch of 3 blank rice samples was spiked with AFB1 standards at concentrations of 2, 5, and 10 $\mu\text{g/kg}$, respectively. After being kept in darkness overnight at room temperature, spiked samples with full organic solvent evaporation and adequate matrix equilibrium were produced. The amounts of AFB1 were measured using the previously calibrated equation, and recoveries were calculated by comparing the measured concentration to the matching spiking quantity. Furthermore, intra-day precision was determined by identifying spiked rice samples within a single day, whereas inter-day precision was independently assessed across six distinct days.

3. Results and discussion

3.1. Preparation and characterization of magnetic rice husk carbon sorbents

As shown in Fig. S1, the MRHC particle dimensions varied within a range of 255.0 nm to 396.06 nm, with a notable peak observed at 341.99 nm, accounting for the greatest proportion of 43.98 % among the entire particle population. The mean diameter was approximately

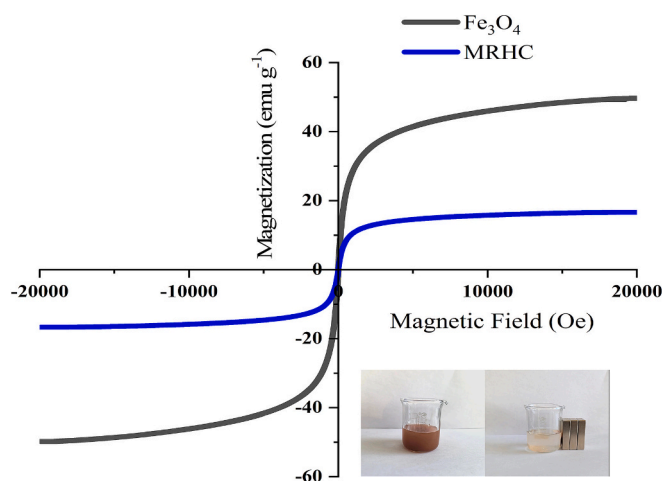


Fig. 2. Magnetization curves of Fe_3O_4 and MRHC.

337.60 nm. The distribution range and average diameter of the Fe_3O_4 particles were significantly lower than those of the MRHC. The nitrogen adsorption-desorption isotherm of MRHC, shown in Fig. S2a, exhibits the characteristics of a Langmuir type IV isotherm. Additionally, the BET specific surface area of MRHC was determined to be $374.83\text{ m}^2/\text{g}$, with a pore size of 3.41 nm (Fig. S2b). The pore size of MRHC is larger than the molecular dimensions of AFB1 ($0.853 \times 1.175 \times 1.484\text{ nm}$), enabling AFB1 to freely enter its porous channel (Li, Zhou, et al., 2022).

The magnetic properties of Fe_3O_4 and MRHC are shown in Fig. 2. Notably, the absence of hysteresis loops within the magnetic profiles of the Fe_3O_4 and MRHC signified their superparamagnetic nature. Specifically, Fe_3O_4 attained a saturation magnetization of 49.32 emu/g, whereas MRHC exhibited a marginally reduced saturation magnetization of 16.32 emu/g. However, MRHC retained sufficient magnetic strength to be swiftly isolated from an aqueous medium using an external magnetic field, as confirmed by the magnetic separation diagram at the bottom-right of Fig. 2.

Fig. 3a shows the XRD profiles of MRHC. The broad diffraction peak observed at 2θ values ranging from 15° to 30° is characteristic of an amorphous material. In this case, the peak suggested the presence of an amorphous SiO_2 structure within the MRHC. Amorphous SiO_2 is known for its lack of long-range order in its atomic arrangement, leading to a diffuse scattering pattern in XRD (Li et al., 2020). The XRD profiles showed several sharp diffraction peaks at specific 2θ angles: 30.26° , 35.60° , 43.30° , 53.80° , 57.42° , and 62.88° . These peaks correspond to the (220), (310), (400), (422), (511), and (440) crystallographic planes of Fe_3O_4 , respectively (Ma et al., 2023). This indicates that the Fe_3O_4 nanoparticles were successfully incorporated into the MRHC after the hydrothermal reaction.

Fig. 3b shows the infrared spectra of Fe_3O_4 with MRHC. The FT-IR spectra of MRHC revealed many absorption peaks (3431 , 1630 , 1089 , 962 , 799 , 467 , and 560 cm^{-1}) that were consistent with prior research (Li, Zhou, et al., 2022). The principal absorption peaks exhibited by MRHC at 3431 and 1630 cm^{-1} could be attributed to the vibrational stretching and bending modes of O—H bonds, respectively (Khalid et al., 2022). The spectral features observed at (1089 , 799 , and 467 cm^{-1}) correspond to the stretching, flexing, and rocking motions of Si—O, whereas the peak at 962 cm^{-1} corresponds to the flexural vibration of Si—OH (Xiong et al., 2020). Furthermore, the vibrational spectra of MRHC at 560 cm^{-1} and Fe_3O_4 at 580 cm^{-1} are both correlated with the telescopic vibrational modes of Fe—O, indicating that Fe—O has successfully combined with RHC to form MRHC, which is in agreement with the XRD results.

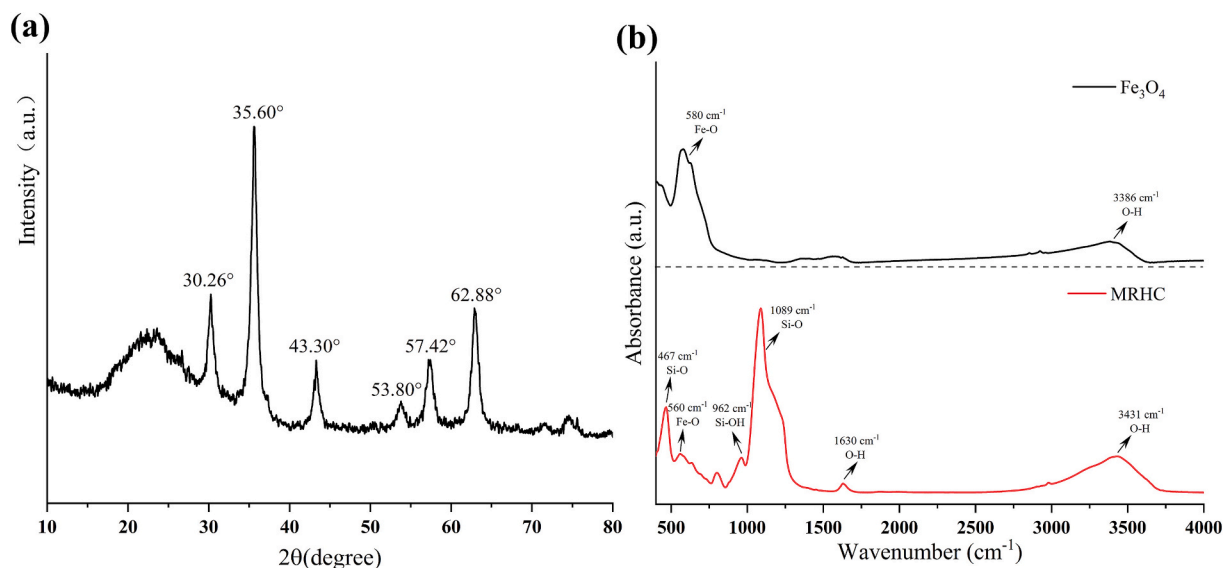


Fig. 3. X-ray diffraction of MRHC (a); FT-IR spectra of Fe_3O_4 and MRHC (b).

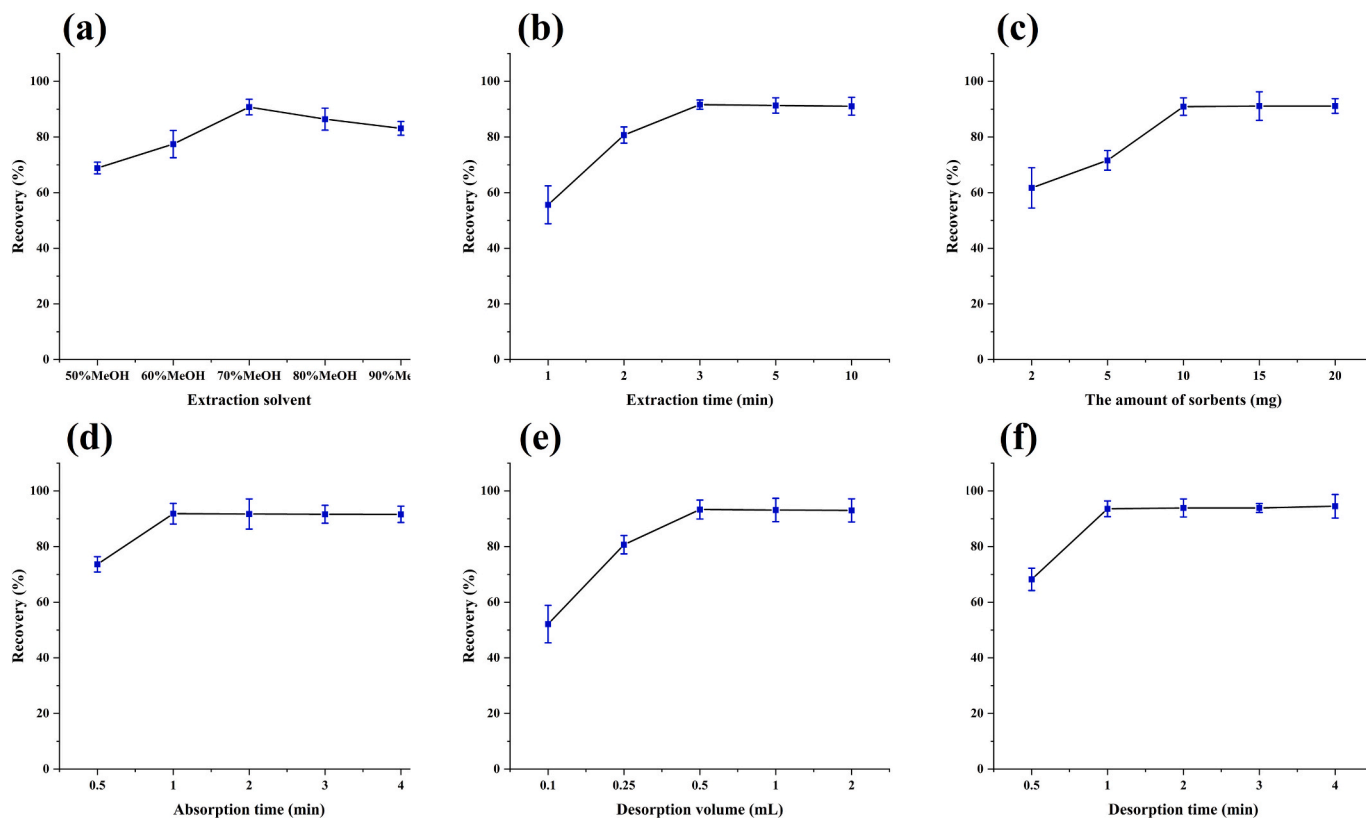


Fig. 4. Optimized MSPE conditions: (a) extraction solvent, (b) extraction time, (c) the amount of sorbents, (d) adsorption time, (e) desorption volume (f) desorption time. Experimental conditions: spiked concentration of AFB1, 5 $\mu\text{g}/\text{kg}$; extractant, 2 mL of 70 % methanol; extraction time, 3 min; amount of adsorbent, 10 mg; adsorption time, 3 min; eluent, 1 mL of methanol; elution time, 1 min. For each parameter, it was optimized with other parameters keeping constant.

3.2. Optimization of MSPE

Before the MSPE, the MRHC was activated by vortexing with dichloromethane for 2 min. After the activation of MRHC, the recovery of AFB1 increased from 21.85 % to 80.27 % (Table S1) and the residual solvent-liquid film allowed AFB1 to penetrate the adsorbent, resulting in improved extraction efficiency and further removal of impurities adsorbed on MRHC.

To further increase MSPE efficiency, diverse parameters influencing extraction efficiency were investigated, including extraction conditions, adsorption conditions, and desorption conditions. Utilizing blank rice samples spiked with AFB1 at a predetermined concentration of 5 $\mu\text{g}/\text{kg}$, the MSPE performance was investigated under varying circumstances. To ensure the precision and optimization of these critical parameters, all experiments were performed in triplicate, and the mean values were calculated.

3.2.1. Extraction conditions

To obtain adequate recovery, several extraction solvent concentrations ranging from 50 % to 90 % MeOH, were investigated. As shown in Fig. 4a, the recovery of AFB1 increased progressively when the concentration of MeOH increased to 70 %. The polarity of the extractant was a significant factor that might enhance the quantity of the analyte (Yuan et al., 2024). The results indicated that 70 % MeOH exhibited the most favorable polarity for the extraction of AFB1, therefore, it was chosen as the extractant.

Adequate extraction was essential for the subsequent steps of MSPE, therefore, the effect of extraction time on MSPE was investigated. The extraction time was varied from 1 to 10 min by vortexing. As shown in Fig. 4b, the AFB1 recovery gradually increased within the initial 3 min of extraction. Beyond this point, an increase in the extraction time led to a negligible change in recovery. This may be due to prolonged extraction, and the mass transfer process essentially reaching equilibrium. (Akamine et al., 2021). Therefore, 3 min was determined as the optimal extraction time.

3.2.2. Adsorption conditions

The amount of MSPE sorbent used for the adsorption varied between 2 and 20 mg. As illustrated in Fig. 4c, the recovery of AFB1 significantly increased from 2 to 10 mg, with slight fluctuations observed between 10 and 20 mg. The small mean diameter of the MRHC particles (337.60 nm) resulted in a large specific surface area, which facilitated the efficient adsorption of AFB1. The rapid adsorption achieved with fewer MSPE sorbents can be attributed to their high dispersity and affinity for AFB1 (Zhou et al., 2017). Thus, 10 mg of MSPE sorbent was determined to be sufficient for extracting and purifying the analytes from the rice samples.

In addition, Fig. 4d shows the adsorption time from 0.5 to 4 min. The findings showed that the mass transfer process between the MRHC and the analyte was completed within 1 min of adsorption. The magnetic extraction procedure was quickly accomplished because of the superparamagnetic properties and excellent dispersibility.

3.2.3. Desorption conditions

The influence of desorption volume was investigated using MeOH spanning from 0.1 up to 2 mL. As shown in Fig. 4e, methanol (0.5 mL) was an efficient desorbent for extracted AFB1 from MRHC. When a greater amount of methanol was used, the recovery remained practically consistent (Yuan et al., 2020). Ultimately, the optimal volume of the desorption solvent was set at 0.5 mL.

An appropriate desorption time is required to ensure complete elution of analytes from adsorbents (Oliveira et al., 2022). Therefore, a series of desorption cycles, ranging from 0.5 to 4 min, were tested. As demonstrated in Fig. 4f, analyte recovery increased as the desorption duration increased from 0.5 to 1 min and remained almost constant, without extending the desorption time. Consequently, the experimental time was set to 1 min.

3.3. Adsorption performance of MRHC

The unit adsorption capacity and adsorption rate of MRHC for AFB1 were investigated at a controlled temperature of 25 °C. Rice extract dilution containing 2 µg/mL AFB1 was used as the adsorption medium for the experiment. Several adsorption time points (0.5, 1, 5, 10, 15, 30, 45, 60, 90, 120, 150, and 200 min) were set, and the unit adsorption capacity of MRHC for AFB1 was determined at each of these time points. Fig. S3 depicts the kinetic characteristics of AFB1 adsorption on MRHC, revealing that its adsorption can be clearly divided into two phases: a fast adsorption phase and a slow adsorption phase. Specifically, at the beginning of the adsorption process (0–30 min), the unit adsorption capacity rapidly increased with time; this phase was defined as the fast adsorption phase. Subsequently, from 30 min until the end of the experiment, the increase in the unit adsorption capacity decreased significantly and the slow adsorption phase began. After 120 min, the

Table 1

The linear range, calibration equation, correlation coefficient, limit of detection (LOD) and limit of quantification (LOQ) for AFB1.

Analyte	Linear range (µg/kg)	Regression equation	R ²	LOD (µg/kg)	LOQ (µg/kg)
AFB1	0.50–25.0	$y = -0.406 \times x + 2.142$	0.9969	0.16	0.50

Table 2

Recoveries and precisions for the determination of AFB1 in rice samples ^a.

Rice samples	Spiked amount (µg/kg)	Recovery (% , n = 6)	Intra-day precision (RSD % , n = 6)	Inter-day precision (RSD % , n = 6)
White rice	2	109.4 ± 8.2	10.7	9.4
	5	91.7 ± 5.7	6.1	8.7
	10	88.1 ± 4.1	8.3	6.8
Glutinous rice	2	94.6 ± 4.9	7.8	11.5
	5	90.9 ± 7.2	4.3	9.2
	10	85.2 ± 5.6	6.8	8.4
Brown rice	2	98.7 ± 8.9	9.1	11.3
	5	93.5 ± 5.3	6.1	10.9
	10	90.6 ± 6.6	5.6	9.7

^a Recoveries, intra-day and inter-day precisions were investigated as mean value in sextuplicate analysis.

adsorption process achieved a maximum unit adsorption capacity of 1.46 mg/g. Concurrently, the adsorption rate peaked, indicating that the adsorption process had reached saturation. MRHC exhibited a higher adsorption capacity for AFB1 than most other carbon materials reported in the literature, although it did not reach the highest reported value. Compared to the adsorption capacities reported in the literature, the adsorption capacity of MRHC was higher than those for most other carbon materials, albeit not reaching the highest reported value. (Asghar et al., 2018; González-Jartín et al., 2019; Ji & Xie, 2021; Ma et al., 2023).

3.4. Method validation

To assess the analytical capabilities of the MSPE grounded in the MRHC, a series of performances were tested under the optimal conditions. This evaluation encompasses several key performance indicators, including capacity, linear range, LOD, accuracy, and repeatability. The adsorptive capability of MRHC for AFB1 was investigated using a previously reported approach with modifications. Different amounts of AFB1 in aqueous medium were extracted and purified, necessitating an excess of AFB1 to be loaded onto the MSPE sorbent. Subsequently, the quantity of the AFB1 adsorbed was quantified using HPLC-FLD. The results indicate that when 10 mg of the MRHC adsorbent was used for the MSPE procedure, AFB1 had a maximum adsorption capacity of approximately 1471.9 ng.

Plotting the proportionate values of the T line to the C line against the logarithmic transformation of the respective concentrations allowed the establishment of a calibration equation for AFB1. Table 1 shows that for AFB1, satisfactory linearity was obtained with acceptable coefficients (R²) of up to 0.9969, spanning from 0.50 to 25 µg/kg. The visual LOD for AFB1 was determined to be 0.16 µg/kg. As shown in Table 2, good recoveries were performed, spanning a range between 85.2 % to 109.4 %. To further examine intra- and inter-day precision, rice samples were spiked with low, medium, and high concentrations of AFB1 on a single day and across six different days. The optimized method exhibited intra-day precision and inter-day precision values that did not exceed 10.7 % and 11.5 %, respectively, demonstrating the good reproducibility of the proposed analytical method.

In addition, the reusability of the MRHC adsorbents was evaluated. As can be seen in Fig. S4, after five adsorption and desorption cycles, the recoveries of AFB1 varied slightly but remained above 83.7 %, which

Table 3

Comparison with the reported method for the determination of aflatoxins.

Sample	Analytes	Pretreatment procedure	Extraction time	Determination method	LODs ($\mu\text{g}/\text{kg}$)	Advantages & limitations	Reference
Corn flour, wheat flour, crab roe	AFB1	Liquid to solid extraction	45 min	Indirect competitive enzymelinked immunosorbent assay (icELISA)	0.18	Rapid, sensitivity and reliable but tedious steps during testing	(Cao et al., 2024)
Cereals, peanut, etc.	AFB1	IAC	50 min	UPLC-MS/MS	0.01–0.06	Sensitivity and efficient but the immune adsorbents are expensive	(Xie et al., 2015)
Peanut	AFB1	Liquid to solid extraction	20 min	Immunochromatographic analysis	1	Rapid and simple but but achieve low sensitivity	(Yuan et al., 2024)
Vegetable oil	AFB1	Low temperature clean-up (LTC) and IMSPE	20 h	Fluorometric analysis	0.0048	Sensitivity, cost-effective but time-consuming	(Yu et al., 2019)
Milk, edible oil, rice	AFB1, AFB2, AFG1, AFG2	MSPE	20 min	LC-MS/MS	0.01–0.05	Rapid and sensitivity but need sophisticated apparatus	(Li, Xu, et al., 2022)
Cereal crops	AFB1, AFB2, AFG1, AFG2	SPE	40 min	HPLC-FLD	0.3–1	Simple and rapid but require using large volumes of organic solvents	(Yu et al., 2018)
Rice	AFB1	MSPE	15 min	TRFICA	0.16	Simple, rapid, sensitivity and cost-effective	This work

indicates that MRHC can be used as an ideal adsorbent for AFB1.

3.5. Application

To assess the feasibility and suitability of the MSPE-TRFICA approach, it was employed for the analysis of AFB1 in a collection of 30 rice samples sourced from the local marketplace. To ensure accuracy, rigorous quality control measures were implemented for the spiked rice blends. A matrix-matched calibration equation was embedded within the portable analytical device to facilitate precise quantification of AFB1 in all rice samples. As is evident from the data presented in Table S2, no AFB1 was detected in these samples.

Table 3 presents a comparison of the proposed approach with previously published methods that analyzed aflatoxins in foods based on factors such as pretreatment procedure, extraction time, determination method, and LODs. Given the inherent complexity of the sample matrix coupled with the low concentration of analytes, streamlining the sample pretreatment process and the analytical procedure is paramount for achieving accurate results. The entire MSPE-TRFICA process could be completed swiftly in 15 min. The sensitivity of the proposed method is comparable to that of LC-MS/MS, HPLC, ELISA, and other established techniques for aflatoxins analysis. Notably, while the achieved LOD is not the lowest among published methodologies, the method facilitated on-site determination of the target compound without the necessity of large, costly inspection equipment. Furthermore, rice samples were spiked with various concentrations of AFB1 for quantification purposes, utilizing both the proposed methodology and the established reference methodology. Congruent findings between the two approaches are shown in Fig. S5. ($y = 0.9567 \times x + 0.1926$, $R^2 = 0.9801$).

The MSPE-TRFICA method offers numerous advantages such as straightforward manipulability, sensitivity, economic efficiency, simple preprocessing procedures, and elimination of the need for detection equipment. This novel method uses MRHC adsorbents conjugated with TRFICA to simplify and expedite the entire operation within 15 min with high accuracy and recovery. The method is suitable for routinely quantifying AFB1 in rice samples. In future studies, we intend to conduct comprehensive field application tests to rigorously assess the stability and reproducibility of this novel methodology across various environmental conditions. The objective of these tests is to meet the regulatory approval criteria necessary for their incorporation into routine agricultural testing procedures.

4. Conclusion

In this study, magnetic rice-husk carbon adsorbents were prepared

with good adsorption capacity for AFB1. The MSPE-TRFICA method was established for the analysis of AFB1 using magnetic rice-husk carbon adsorbents as effective adsorbents for the first time. Under optimal settings, the LOD for AFB1 was determined to be 0.16 $\mu\text{g}/\text{kg}$. The experimental results demonstrate that the entire proposed method can be implemented within 15 min with high quantitative precision, good recovery, and high efficiency. Hence, the proposed method based on a magnetic rice-husk carbon adsorbent can be successfully applied for the determination of AFB1 in rice samples.

CRediT authorship contribution statement

Di Yuan: Writing – original draft, Visualization, Validation, Software, Resources, Methodology, Investigation, Funding acquisition, Data curation, Conceptualization. **Bin Hong:** Validation, Methodology. **Shan Zhang:** Writing – review & editing, Visualization. **Shan Shan:** Supervision, Investigation. **Jingyi Zhang:** Visualization, Supervision. **Chuan-ying Ren:** Writing – review & editing, Project administration, Funding acquisition.

Declaration of competing interest

The authors declare that they have no known competing financial interests or personal relationships that could have appeared to influence the work reported in this paper.

Acknowledgements

This work was supported by the China Rice Industry Technology System (CARS-01-50), the Heilongjiang Scientific Research Fund Project (CZKYF2023-1-C015), Heilongjiang Key R&D Program Project (JD2023GJ04) and the Innovation Project of Heilongjiang Academy of Agricultural Sciences (CX23YQ07).

Appendix A. Supplementary data

Supplementary data to this article can be found online at <https://doi.org/10.1016/j.fochx.2024.102145>.

Data availability

Data will be made available on request.

References

- Akamine, L. A., Vargas Medina, D. A., & Lanças, F. M. (2021). Magnetic solid-phase extraction of gingerols in ginger containing products. *Talanta*, 222, Article 121683. <https://doi.org/10.1016/j.talanta.2020.121683>
- Amran, M., Fediuk, R., Murali, G., Vatin, N., Karelina, M., Ozbakkaloglu, T., ... Mishra, J. (2021). Rice husk ash-based concrete composites: A critical review of their properties and applications. *Crystals*, 11, 168. <https://doi.org/10.3390/cryst11020168>
- Asadi, H., Ghorbani, M., Rezaei-Rashti, M., Abrishamkesh, S., Amirahmadi, E., Chengrong, C., & Gorji, M. (2021). Application of rice husk biochar for achieving sustainable agriculture and environment. *Rice Science*, 28, 325–343. <https://doi.org/10.1016/j.rsci.2021.05.004>
- Asghar, M. A., Zahir, E., Shahid, S. M., Khan, M. N., Asghar, M. A., Iqbal, J., & Walker, G. (2018). Iron, copper and silver nanoparticles: Green synthesis using green and black tea leaves extracts and evaluation of antibacterial, antifungal and aflatoxin B1 adsorption activity. *LWT*, 90, 98–107. <https://doi.org/10.1016/j.lwt.2017.12.009>
- Bai, Y., Jiang, H., Zhang, Y., Dou, L., Liu, M., Yu, W., ... Wang, Z. (2021). Hydrophobic moiety of capsaicinoids haptens enhancing antibody performance in immunoassay: Evidence from computational chemistry and molecular recognition. *Journal of Agricultural and Food Chemistry*, 69, 9957–9967. <https://doi.org/10.1021/acs.jafc.1c03657>
- Bhat, S. A., Sher, F., Hameed, M., Bashir, O., Kumar, R., Vo, D.-V. N., ... Lima, E. C. (2022). Sustainable nanotechnology based wastewater treatment strategies: Achievements, challenges and future perspectives. *Chemosphere*, 288, Article 132606. <https://doi.org/10.1016/j.chemosphere.2021.132606>
- Cao, J., Wang, T., Wu, K., Zhou, F., Feng, Y., Li, J., & Deng, A. (2024). A highly sensitive and group-specific enzyme-linked immunosorbent assay (ELISA) for the detection of AFB1 in agriculture and aquaculture products. *Molecules*, 29, 2280. <https://doi.org/10.3390/molecules29102280>
- Chandrayarnan, P., Agyei, D., & Ali, A. (2024). The prevalence and concentration of mycotoxins in rice sourced from markets: A global description. *Trends in Food Science & Technology*, 146, Article 104394. <https://doi.org/10.1016/j.tifs.2024.104394>
- González-Jartín, J. M., de Castro Alves, L., Alfonso, A., Piñeiro, Y., Vilar, S. Y., Gomez, M. G., ... Botana, L. M. (2019). Detoxification agents based on magnetic nanostructured particles as a novel strategy for mycotoxin mitigation in food. *Food Chemistry*, 294, 60–66. <https://doi.org/10.1016/j.foodchem.2019.05.013>
- Hong, R., Li, J., Li, H., Ding, J., Zheng, Y., & Wei, D. (2008). Synthesis of Fe₃O₄ nanoparticles without inert gas protection used as precursors of magnetic fluids. *Journal of Magnetism and Magnetic Materials*, 320, 1605–1614. <https://doi.org/10.1016/j.jmmm.2008.01.015>
- Hu, S., Dou, X., Zhang, L., Xie, Y., Yang, S., & Yang, M. (2018). Rapid detection of aflatoxin B1 in medicinal materials of radix and rhizome by gold immunochromatographic assay. *Toxicol*, 150, 144–150. <https://doi.org/10.1016/j.toxicol.2018.05.015>
- Huang, Q., Lin, X., Chen, D., & Tong, Q. (2022). Carbon dots/α-Fe₂O₃-Fe₃O₄ nanocomposite: Efficient synthesis and application as a novel electrochemical aptasensor for the ultrasensitive determination of aflatoxin B1. *Food Chemistry*, 373, Article 131415. <https://doi.org/10.1016/j.foodchem.2021.131415>
- Jallow, A., Xie, H., Tang, X., Qi, Z., & Li, P. (2021). Worldwide aflatoxin contamination of agricultural products and foods: From occurrence to control. *Comprehensive Reviews in Food Science and Food Safety*, 20, 2332–2381. <https://doi.org/10.1111/1541-4337.12734>
- Ji, J., & Xie, W. (2021). Removal of aflatoxin B1 from contaminated peanut oils using magnetic attapulgite. *Food Chemistry*, 339, Article 128072. <https://doi.org/10.1016/j.foodchem.2020.128072>
- Khalid, U., Sher, F., Noreen, S., Lima, E. C., Rasheed, T., Sehar, S., & Amami, R. (2022). Comparative effects of conventional and nano-enabled fertilizers on morphological and physiological attributes of *Caesalpinia bonducella* plants. *Journal of the Saudi Society of Agricultural Sciences*, 21, 61–72. <https://doi.org/10.1016/j.jssas.2021.06.011>
- Lai, X., Zhang, H., Liu, R., & Liu, C. (2015). Potential for aflatoxin B1 and B2 production by *Aspergillus flavus* strains isolated from rice samples. *Saudi Journal of Biological Sciences*, 22, 176–180. <https://doi.org/10.1016/j.sjbs.2014.09.013>
- Li, J., Xu, X., Guo, W., Zhang, Y., Feng, X., & Zhang, F. (2022). Synthesis of a magnetic covalent organic framework as sorbents for solid-phase extraction of aflatoxins in food prior to quantification by liquid chromatography-mass spectrometry. *Food Chemistry*, 387, Article 132821. <https://doi.org/10.1016/j.foodchem.2022.132821>
- Li, R., Zhang, M., Fu, X., Gao, J., Huang, C., & Li, Y. (2022). Research of low-dimensional carbon-based magnetic materials. *ACS Applied Electronic Materials*, 4, 3263–3277. <https://doi.org/10.1021/acsaem.2c00407>
- Li, Y., Wang, R., Chen, Z., Zhao, X., Luo, X., Wang, L., ... Teng, F. (2020). Preparation of magnetic mesoporous silica from rice husk for aflatoxin B1 removal: Optimum process and adsorption mechanism. *PLoS One*, 15, Article e0238837. <https://doi.org/10.1371/journal.pone.0238837>
- Li, Y., Zhou, Y., Wang, R., Chen, Z., Luo, X., Wang, L., Zhao, X., Zhang, C., & Yu, P. (2022). Removal of aflatoxin B1 from aqueous solution using amino-grafted magnetic mesoporous silica prepared from rice husk. *Food Chemistry*, 389, Article 132987. <https://doi.org/10.1016/j.foodchem.2022.132987>
- Ma, F., Guo, Q., Zhang, Z., Ding, X., Zhang, L., Li, P., & Yu, L. (2023). Simultaneous removal of aflatoxin B1 and zearalenone in vegetable oils by hierarchical fungal mycelia@graphene oxide/Fe₃O₄ adsorbent. *Food Chemistry*, 428, Article 136779. <https://doi.org/10.1016/j.foodchem.2023.136779>
- Muthukumar, P., Suresh Babu, P., Shyamalagowri, S., Aravind, J., Kamaraj, M., & Govarthanan, M. (2022). Polymeric biomolecules based nanomaterials: Production strategies and pollutant mitigation as an emerging tool for environmental application. *Chemosphere*, 307, Article 136008. <https://doi.org/10.1016/j.chemosphere.2022.136008>
- Oliveira, R. V. M., Santos, A. F., Santos, M. D. L., Cunha, G. D. C., & Romão, L. P. C. (2022). Magnetic solid-phase extraction of bisphenol A from water samples using nanostructured material based on graphene with few layers and cobalt ferrite. *Microchemical Journal*, 181, Article 107741. <https://doi.org/10.1016/j.microc.2022.107741>
- Özdemir, S., Mohamedsaid, S. A., Kılınc, E., & Soyak, M. (2019). Magnetic solid phase extractions of Co(II) and Hg(II) by using magnetized C. Micaceous from water and food samples. *Food Chemistry*, 271, 232–238. <https://doi.org/10.1016/j.foodchem.2018.07.067>
- Senosy, I. A., Guo, H., Ouyang, M., Lu, Z., Yang, Z., & Li, J. (2020). Magnetic solid-phase extraction based on nano-zeolite imidazolate framework-8-functionalized magnetic graphene oxide for the quantification of residual fungicides in water, honey and fruit juices. *Food Chemistry*, 325, Article 126944. <https://doi.org/10.1016/j.foodchem.2020.126944>
- Somsunsin, S., Seebunrueng, K., Boonchiangma, S., & Srijaranai, S. (2018). A simple solvent based microextraction for high performance liquid chromatographic analysis of aflatoxins in rice samples. *Talanta*, 176, 172–177. <https://doi.org/10.1016/j.talanta.2017.08.028>
- Syuhada, A., Ameen, M., Azizan, M. T., Aqsha, A., Yusoff, M. H. M., Ramli, A., ... Sher, F. (2021). In-situ hydrogenolysis of glycerol using hydrogen produced via aqueous phase reforming of glycerol over sonochemically synthesized nickel-based nanocatalyst. *Molecular Catalysis*, 514, Article 111860. <https://doi.org/10.1016/j.mcat.2021.111860>
- Urusov, A. E., Zherdev, A. V., & Dzantiev, B. B. (2019). Towards lateral flow quantitative assays: Detection approaches. *Biosensors*, 9, 89. <https://doi.org/10.3390/bios9030089>
- Wu, W., Bai, Y., Zhao, T., Liang, M., Hu, X., Wang, D., ... Zhang, Z. (2023). Intelligent electrochemical point-of-care test method with interface control based on DNA pyramids: Aflatoxin B1 detection in food and the environment. *Foods*, 12, 4447. <https://doi.org/10.3390/foods12244447>
- Xie, J., Peng, T., He, J., Shao, Y., Fan, C., Chen, Y., Jiang, W., Chen, M., Wang, Q., Pei, X., Ding, S., & Jiang, H. (2015). Preparation and characterization of an immunoaffinity column for the selective extraction of aflatoxin B1 in 13 kinds of foodstuffs. *Journal of Chromatography B*, 998–999, 50–56. <https://doi.org/10.1016/j.jchromb.2015.06.022>
- Xiong, J., Li, G., & Hu, C. (2020). Treatment of methylene blue by mesoporous Fe/SiO₂ prepared from rice husk pyrolytic residues. *Catalysis Today*, 355, 529–538. <https://doi.org/10.1016/j.cattod.2019.06.059>
- Yu, L., Ma, F., Ding, X., Wang, H., & Li, P. (2018). Silica/graphene oxide nanocomposites: Potential adsorbents for solid phase extraction of trace aflatoxins in cereal crops coupled with high performance liquid chromatography. *Food Chemistry*, 245, 1018–1024. <https://doi.org/10.1016/j.foodchem.2017.11.070>
- Yu, X., Keitel, C., & Dijkstra, F. A. (2021). Global analysis of phosphorus fertilizer use efficiency in cereal crops. *Global Food Security*, 29, Article 100545. <https://doi.org/10.1016/j.gfs.2021.100545>
- Yu, X., Li, Z., Zhao, M., Lau, S. C. S., Ru Tan, H., Teh, W. J., ... Zhang, Y. (2019). Quantification of aflatoxin B1 in vegetable oils using low temperature clean-up followed by immuno-magnetic solid phase extraction. *Food Chemistry*, 275, 390–396. <https://doi.org/10.1016/j.foodchem.2018.09.132>
- Yuan, B., Liu, Q., Yang, Q., Pang, C., Xu, H., Du, X., Wei, L., Nie, K., Guo, Y., & Sun, X. (2024). An immediate and antibody protected carboxyl quantum dot immunochromatographic analysis hierarchical signal amplification test strip based on biotin-streptavidin system for the detection of aflatoxin B1 in peanuts. *Journal of Food Composition and Analysis*, 125, Article 105759. <https://doi.org/10.1016/j.jfca.2023.105759>
- Yuan, D., Li, S., Zhang, L., Ma, F., Wang, H., Zhang, Q., & Li, P. (2023). Rapid and sensitive quantification of capsaicinoids for edible oil adulteration by immunomagnetic solid-phase extraction coupled with time-resolved fluorescent immunochromatographic assay. *Food Chemistry*, 404, Article 134552. <https://doi.org/10.1016/j.foodchem.2022.134552>
- Yuan, D., Yuan, Y., Zhang, L., Ma, F., & Li, P. (2024). Rapid, efficient, and accurate determination of aflatoxins and capsaicinoids in vegetable oils by immunomagnetic sorbents coupled with UHPLC-MS/MS. *Food Frontiers*, 5, 1004–1013. <https://doi.org/10.1002/fft2.382>
- Yuan, Y., Wu, Y., Wang, H., Tong, Y., Sheng, X., Sun, Y., Zhou, X., & Zhou, Q. (2020). Simultaneous enrichment and determination of cadmium and mercury ions using magnetic PAMAM dendrimers as the adsorbents for magnetic solid phase extraction coupled with high performance liquid chromatography. *Journal of Hazardous Materials*, 386, Article 121658. <https://doi.org/10.1016/j.jhazmat.2019.121658>
- Zafar, N., Niazi, M. B. K., Sher, F., Khalid, U., Jahan, Z., Shah, G. A., & Zia, M. (2021). Starch and polyvinyl alcohol encapsulated biodegradable nanocomposites for environment friendly slow release of urea fertilizer. *Chemical Engineering Journal Advances*, 7, Article 100123. <https://doi.org/10.1016/j.cej.2021.100123>
- Zhou, Q., Lei, M., Liu, Y., Wu, Y., & Yuan, Y. (2017). Simultaneous determination of cadmium, lead and mercury ions at trace level by magnetic solid phase extraction with Fe@ag-Dimercaptobenzene coupled to high performance liquid chromatography. *Talanta*, 175, 194–199. <https://doi.org/10.1016/j.talanta.2017.07.043>